ELSEVIER

Journal of Power Sources 78 (1999) 115–122

JOURNAL OF POWER SOURCES

Bipolar lead/acid batteries: effect of membrane conductivity on performance

M. Coux [a,*], X. Muneret [a], P. Lenain [a], J.L. Wojkiewicz [b], J. Renard [c]

[a] *OLDHAM France, Service Technique, 62033 Arras Cedex, France*
[b] *Ecole des Mines de Douai, Laboratoire Polymère Conducteur, 59508 Douai cedex, France*
[c] *Ecole des Mines de Paris, Centre des Matériaux Pierre et Marie Fourt, 91003 Evry Cedex, France*

Abstract

Bipolar lead/acid batteries offer the possibility of increased energy and power density. This paper presents the results of a theoretical and experimental study into the performance of a bipolar construction. A model that calculates the ohmic losses in a bipolar lead acid battery has been used to predict the cell voltage during discharge. The calculated discharge curves are in good agreement with experimental results obtained with a 6 V lead membrane bipolar prototype. In a second part the conductivity of the bipolar plates have been adjusted in the program to estimate its influence on battery performance.

Keywords: Bipolar lead/acid battery; Modelling; Potential distribution

1. Introduction

The use of the bipolar design Fig. 1 is certainly the best way to improve the specific energy of a lead/acid cell. It presents two basic advantages compared with grid designs. The ohmic losses between positive and negative active material are lower. This allows the use of less conductive composites that can greatly reduce the battery weight. Because of the frontal collection of electrical charges, the current distribution is uniform and active materials work more homogeneously. This results in an improvement of the battery efficiency. Nevertheless, as the conductivity of the bipolar membrane decreases, the voltage distribution becomes less and less uniform and if conductivity is too low, the performance will be limited. The calculation of voltage distribution in the bipolar stack allows this limit to be determined. Very few papers deal with bipolar lead acid battery modelling. Wen-Hong [1], whose program is an extension of that introduced by Tiedemann and Newman [2], studies the influence of the membrane or active material thickness and discharge rate on bipolar lead/acid battery performance. Scott [3] calculated the current distribution in a bipolar assembly. The battery is modelled by a stack of materials of different resistivities. He analytically solved the problem for some specific cases. This approach does not apply in a general case and furthermore, it does not take into account electrochemical aspects. Mao and White [4] calculated the voltage distribution for the HORIZON® quasi bipolar lead/acid battery. The Butler Volmer expression is used to describe electrochemical overvoltage and they solved the equation with a finite element method.

Potential distribution has been calculated by some authors in the standard case of grid design but not for bipolar design. Morimoto et al. [5] presents a model where potential distribution is calculated from grid resistivity and experimental polarisation data. After calculating the potential distribution for one state of charge, he simulates the whole discharge by adjusting each battery component resistivity. Sunu and Burrows [6,7] have a similar approach, at first, they modeled the grid as a resistive network and calculate the associated potential distribution. They adjusted the resistivity of each component to simulate the discharge. In this case electrochemical overvoltage evolution is neglected.

We have developed a model to calculate the current and potential distribution in the case of a bipolar stack. This allows the study of influence of both membrane conductiv-

* Corresponding author

0378-7753/99/$ - see front matter
PII: S0378-7753(99)00020-8

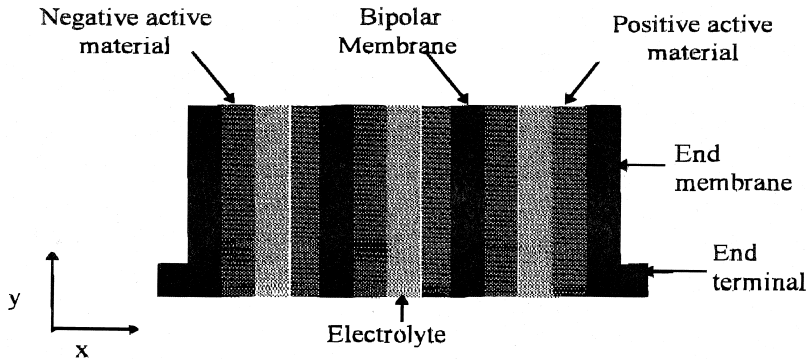

Fig. 1. Schematic diagram of a polar lead acid cell.

ity and rate of discharge on battery efficiency. The method is similar to that used by Morimoto et al. or Sunu and Burrows but in the case of a bipolar stack. A resistive matrix representative of the battery is calculated for each step of discharge. The calculation of the voltage distribution is based on this matrix, using the Gauss Seidel method. The Butler Volmer expression is used as a model for charge transfer overvoltage and a specific calculation is made to introduce the influence of diffusion in this expression.

2. Mathematical model

For each state of charge the overall battery voltage is considered to be the difference between the equilibrium voltage and both ohmic losses and electrochemical overvoltages.

The battery is represented by a resistive network. A two dimensional mesh is applied on a plane that crosses the end terminals.

The resistivity of each component in this matrix that represents the battery is reported. An additional resistive term is used to simulate the effect of electrochemical phenomena. This term is introduced in the resistive matrix, at the interface between the active material and the electrolyte. This matrix and the discharge current are used to calculate the potential distribution.

2.1. Fundamental equations

Assuming that a discharge is a succession of steady states, governing laws are: conservation of electrical charge at each point: Div $\vec{j} = 0$ with $\vec{j} = \vec{j}_x + \vec{j}_y$ resulting in

$$\frac{\delta j_x}{\delta x} + \frac{\delta j_y}{\delta y} = 0 \tag{1}$$

Ohm's law can be written: $\vec{j} = \sigma \vec{\mathscr{E}}$ but as $\vec{\mathscr{E}} = -\mathrm{grad}\vec{V}$ the current density becomes:

$$j_x = -\sigma \frac{\delta V}{\delta x} \quad j_y = -\sigma \frac{\delta V}{\delta y} \tag{2}$$

where: j, current density (A cm^{-2}); V, voltage (V); σ, conductivity (S cm^{-1}); E, electrical field (V cm^{-1})

The equation to give the result is:

$$\frac{\delta\left(\sigma(x,y)\dfrac{\delta V(x,y)}{\delta x}\right)}{\delta x} + \frac{\delta\left(\sigma(x,y)\dfrac{\delta V(x,y)}{\delta y}\right)}{\delta y} = 0 \tag{3}$$

for constant conductivity this equation takes a Laplacian form.

2.2. Resolution

A numerical method is used to solve this problem. The equation has been discretised and partial difference approximated by finite difference. Then the equation to be solved becomes:

$$(a+b+c+d)V_{(i,j)} + aV_{(i+1,j)} + bV_{(i-1,j)} + cV_{(ij+1)} + dV_{(ij-1)} = 0 \tag{4}$$

with:

$$a = \frac{\sigma_i(i+1,j)}{\Delta x^2}, \quad b = \frac{\sigma_i(i,j)}{\Delta x^2}, \quad c = \frac{\sigma_j(i,j+1)}{\Delta y^2},$$

$$d = \frac{\sigma_j(i,j)}{\Delta y^2}$$

This equation was solved by a computer using the Gauss Seidel method that is suitable for elliptic problems. It is an iterative method, the solution calculated at the step k is used to calculate those at step $k+1$. The calculations become:

$$V_{k+1}(i,j) = \frac{aV_k(i+1,j) + bV_k(i-1,j) + cV_k(i,j+1) + dV_k(i,j-1)}{a+b+c+d} \tag{5}$$

The initial distribution potential is calculated assuming that all layers of the stack are equipotential.

3. Electrochemical overvoltages

With this resolution method it is not possible to take into account the electrochemical phenomena directly, therefore, they have been represented by the equivalent ohmic losses through a resistance. This resistance is equal to the ratio of overvoltage on current and it is introduced in series between the active materials and the electrolyte. In this approach, the electrochemical overvoltages over the whole electrode are represented by a single value. It allows calculation of a new potential distribution. By successive iterations, electrochemical overvoltages are correctly taken into account.

3.1. Charge transfer overvoltage

The charge transfer overvoltage can be expressed by the Butler Volmer expression:

$$I = I_0\left[\exp\left(\frac{\alpha nF}{RT}\left(E - E_{eq}\right)\right) - \exp\left(\frac{-\left(I-\alpha\right)nF}{RT}\left(E - E_{eq}\right)\right)\right] \quad (6)$$

where: I, total current (A); I_0, equilibrium current (A); E, electrode potential (V); E_{eq}, Electrode standard potential (V); n, F, R, T have their usual meanings.

The overvoltage is defined as the difference between the equilibrium potential and the electrode potential.

$$\eta_t = E - E_{eq} \quad (7)$$

The charge transfer coefficient α whose value is very close to 0.5 [9] has been replaced by this value in the preceding formula, then:

$$\eta_t = \frac{RT}{nF}\operatorname{arcsinh}\left(\frac{I}{2I_0}\right) \quad (8)$$

this expression establishes a direct link between current and overpotential.

3.2. Penetration length

Because of diffusion, only part of active material takes part in the reaction. It is possible to define a penetration depth beyond which the reaction is negligible. De Levie [8] gave an expression of this length:

$$X_{react} = CD_* \frac{nF}{j\left(I-\varepsilon\right)} \quad (9)$$

where: j, current density (A cm^{-2}); ε, active material porosity (%); C, electrolyte concentration mole cm^{-3}; D_*: Diffusion coefficient inside the active material (cm^2 s^{-1}).

It is considered that, if the thickness of the electrode exceeds this value, the inner part of the active material does not take part in the reaction.

3.3. Diffusion effect

The effect of concentration varies at each point of the electrode, therefore, it is not possible to represent such a phenomenon by a single value. By assuming that the global overvoltage due to the charge transfer and to the diffusion effects remains constant at each point of the electrode (when diffusion effects increase, the reaction and the charge transfer overvoltages decrease) all the electrochemical phenomena are taken into account by a single value.

At the surface of the electrode, electrochemical overvoltage is only due to charge transfer, therefore by calculating the reaction current density j_{max} at the surface of the electrode, it is possible to calculate with the Butler Volmer expression a value that represents overvoltage at each point of the electrode.

A specific calculation has been made to determine the reaction current density distribution all over the electrode.

At first, we can assume that the ratio j/C is constant through the thickness of the electrode, assuming that η remains constant and that the concentration effect can be taken into account in the Butler Volmer expression [9] by the following expression:

$$j(x) = j_0\left(\frac{C(x)}{C_{el}}\right)\left[\exp\left(\frac{nF}{2RT}\eta\right) - \exp\left(-\frac{nF}{2RT}\eta\right)\right] \quad (10)$$

where: C_{el}, bulk electrolyte concentration (mole cm^{-3}); S_S, specific area (cm^2 cm^{-3}); j_0, Equilibrium current density (A cm^{-2}); $j(x)$, reacting current density (A cm^{-2}).

This hypothesis has been used in the following calculation of the concentration profile.

If $N(x)$ is the ionic fluxes at each point, we can write [10]:

$$\frac{\delta N(x)}{\delta x} = \frac{-1}{nF} j(x) S_S \quad (11)$$

The decrease of the ionic flux is due to the part of species that reacts to generate an electrical current in the solid phase of the electrode.

The first Fick law can be written:

$$N(x) = -D\frac{\delta C(x)}{\delta x} \quad (12)$$

$N(x)$, species flux mol cm^{-2} s^{-1}

The equation to be solved is:

$$\frac{\delta^2 C}{\delta x^2} = \frac{l}{nFD} j(x) S_S \quad (13)$$

And $j(x)/C(x)$ is constant, if we take:

$$A = \frac{S_S j_0}{nFDC_{el}}\left(\exp\left(\frac{nF}{2RT}\eta\right) - \exp\left(-\frac{nF}{2RT}\eta\right)\right),$$

we obtain the following equation:

$$\frac{\delta^2 C(x)}{\delta x^2} = AC(x), \tag{14}$$

and with the initial conditions:

$$x = 0, \quad C(0) = 0, \quad x = e, \quad \frac{\delta C}{\delta x} = 0,$$

it results in:

$$C(x) = C_{el}\frac{\left(\exp\left(-\sqrt{Ax}\right) + \exp\left(-2\sqrt{Ae}\right)\exp\left(\sqrt{Ax}\right)\right)}{1 + \exp\left(-2\sqrt{Ae}\right)} \tag{15}$$

the total current density is the sum of the reacting current density all over the electrode thickness:

$$\int_o^c j(x) S_S \, dx = j_{tot}$$

becomes:

$$\frac{j_{tot}}{C_{el} nFD} = \sqrt{A}\,\frac{l - \exp\left(-2\sqrt{Ae}\right)}{l + \exp\left(-2\sqrt{Ae}\right)} \tag{16}$$

.

Using numerical procedures, it is possible to determine A for different values of the total current. The calculated concentrations along the electrode thickness are reported in Fig. 2 for various current densities.

This calculation shows that, as the rate of discharge increases, the electrolyte concentration inside the porous material becomes less uniform and the penetration depth decreases. Furthermore, it allows the definition of the reaction current density j_{max} at the surface of the electrode. It is used in the Butler Volmer expression. The overvoltage value obtained gives a good idea with a single value of both charge transfer and diffusion for all the electrode thicknesses.

4. Evolution during discharge

4.1. Evolution of equilibrium voltage

The equilibrium voltage depends on electrolyte concentration. The average concentration can be easily deduced from the discharged capacity by the following calculation:

$$C = C_i - \frac{3600Q}{nF}\frac{I}{V_{el}} \tag{17}$$

.

Concentration can also be expressed in weight percentage W. In this case, it is deduced from the preceding value:

$$W = 100\frac{M_{H_2SO_4}C}{\left(M_{H_2SO_4}C + M_{H_2O}C_{H_2O}\right)} \tag{18}$$

M, molar mass (g mol^{-1}) with

$$C_{H_2O} = \left(1 - C\frac{M_{H_2SO_4}}{d_{H_2SO_4}}\right)\frac{d_{H_2O}}{M_{H_2O}}$$

This notation is more practical to express the equilibrium voltage dependence:

$$E_{eq} = 1.848 + 7.42 \cdot 10^{-3} W \tag{19}$$

This relation is given by Biscaglia [10] in his thesis and it is close to reality for the 5 to 40 weight percentage range.

The equilibrium voltage is added due to ohmic and electrochemical losses, to obtain the overall voltage of a cell.

4.2. Ohmic conductivity evolution

Lead dioxide conductivity depends on crystalline phase (α or β), and the value varies from one reference to

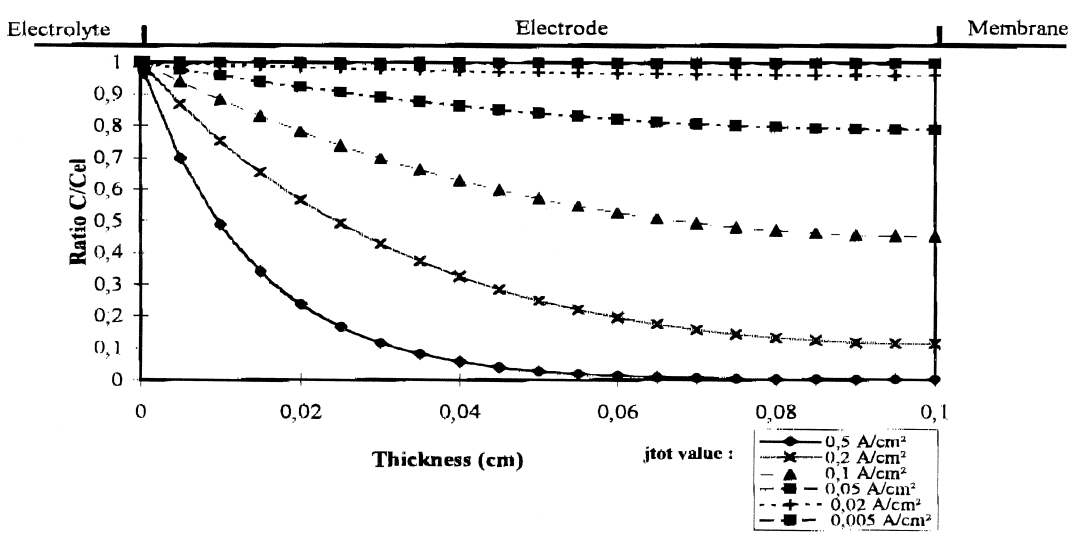

Fig. 2. Electrolyte concentration vs. penetration depth for different values of discharge current density.

Table 1
Evolution of the exponent n in the Peukert relation vs. discharge rate.

Discharge time	Exponent n value
5 h	1.05
1 h	1.099
30 min	1.117
10 min	1.143

another. A value of 200 S cm^{-1} seems correct [10]. Lead conductivity, at the negative electrode, is well defined: $\sigma = 48\,000$ S cm^{-1}.

The active material has a high porosity and the real conductivity can be estimated from its component conductivity by the Bruggeman expression [9,11]:

$$\sigma_{MA} = \sigma(1-\varepsilon)^{1.5} \quad (20)$$

where: ε, active material porosity; σ_{MA}, conductivity of porous active material (S cm^{-1}); σ, conductivity of non-porous material (S cm^{-1}).

The conductivity of active material decreases when the active material reacts to form lead sulphate and the interface between active material and electrolyte progressively becomes insulated. It is usually accepted that this evolution is linear with discharged capacity [7]:

$$\sigma_{MA} = \sigma_{MA,i}\left(1 - \frac{Q}{Q_{tot}}\right) \quad (21)$$

where Q is the electric capacity and Q_{tot} is the reference discharge capacity.

The ionic conductivity of sulphuric acid depends on its concentration and the conductivity vs. weight percentage acid concentration can be fitted by [10]:

$$\sigma_{el} = \sigma_{max}\exp\left(-2.61\cdot 10^{3} W^{-0.288}(W - W_{max})^{2}\right) \quad (22)$$

where σ_{max} (0.76 S cm^{-1}) is the maximum conductivity and W_{max} (31.3%) the concentration percentage at this conductivity.

4.3. Electrochemical overvoltage

During discharge the charge transfer overvoltage steadily increases because of decreasing reacting area due to coverage of active material by sulphate crystals [12,7]:

$$S_S = S_{S,i}\left(1 - \frac{Q}{Q_{tot}}\right) \quad (23)$$

where S_S is the specific area of the fully charged electrode.

The diffusion overvoltage increases too. We have considered that this evolution is mainly due to the decrease in the diffusion coefficient with electrolytic concentration, this coefficient linearly increases with concentration [13]:

$$D = D_i(0.706 + 58.8C), \quad D_i = 7.2\cdot 10^{-6}\ \mathrm{cm^2 s^{-1}} \quad (24)$$

5. Experimental: model validation

The results obtained with the model have been adjusted with experimental data measured with a 6 V, 2.5 A h lead membrane prototype.

Two parameters have been used to fit experimental data.

The reference discharge capacity depends on the rate of discharge because the lead sulphate crystals become smaller and more numerous as the discharge current increases [13] and it causes a decrease in the available capacity because the reacting area will rapidly decrease. The Peukert relation $I^n t = k$ is used to evaluate this capacity for each rate.

The constant k is calculated for the 20 h rate discharge and the exponent n is adjusted for each rate of discharge. The results obtained are reported in Table 1.

The value of this exponent increases with the discharge rate. Therefore, it confirms the hypothesis that, for increas-

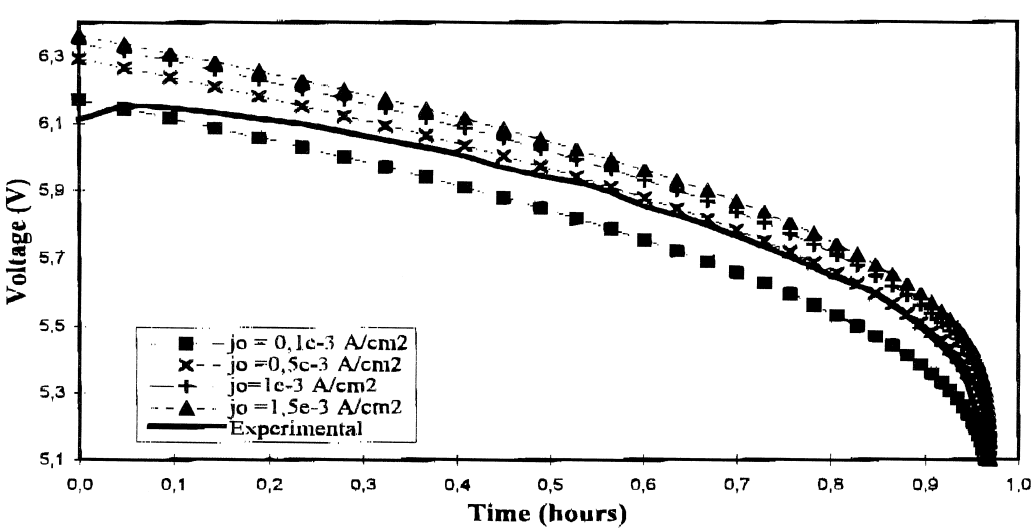

Fig. 3. Model validation for different values of the exchange current density.

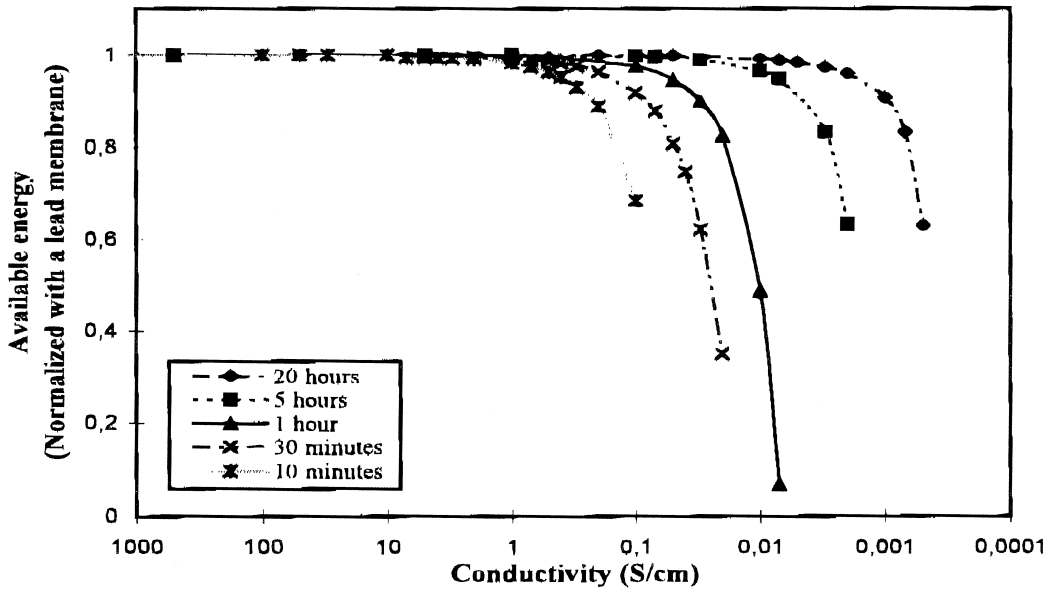

Fig. 4. Available energy vs. membrane conductivity for different rates of discharge and with current uniformly distributed on the end membranes.

ing discharge current, the available capacity is not only limited by diffusion problems but also by evolution of sulphate crystal size.

The exchange current density j_0 is the second parameter used to adjust the model. It is higher for the negative electrode, and the resulting overvoltages are lower than on the positive electrode. So the exchange current density is more significant for the positive electrode. Its value is the only one to have been used to adjust the model. The values of this parameter are not well defined and vary from one reference to another.

Biscaglia uses Bode's [8] value of $0.16.10^{-3}$ A cm^{-2} in calculations. Laffolette considers that the value can range from 0.2 to $2.4 \cdot 10^{-3}$ A cm^{-2} and Dasoyan and Aguf [14] report calculated values that range from 0.015 to $4.9 \cdot 10^{-3}$ A cm^{-2}.

The values used to adjust the model range from $0.1 \cdot 10^{-3}$ to $1.5 \cdot 10^{-3}$ A cm^{-2}. The results obtained for a 30 min discharge are reported on Fig. 3.

The best fit is obtained for $j_0 = 0.5 \cdot 10^{-3}$ A cm^{-2}. This value has been used for the 20 h, the 5 h, the 30 min and the 10 min rates and shows good agreement.

The difference observed at the beginning of the discharge is due to the 'coup de fouet' effect that has not been taken into account.

6. Performance predictions for composite membranes

This model has been used to predict the available energy when the membrane conductivity decreases. Two different cases have been evaluated.

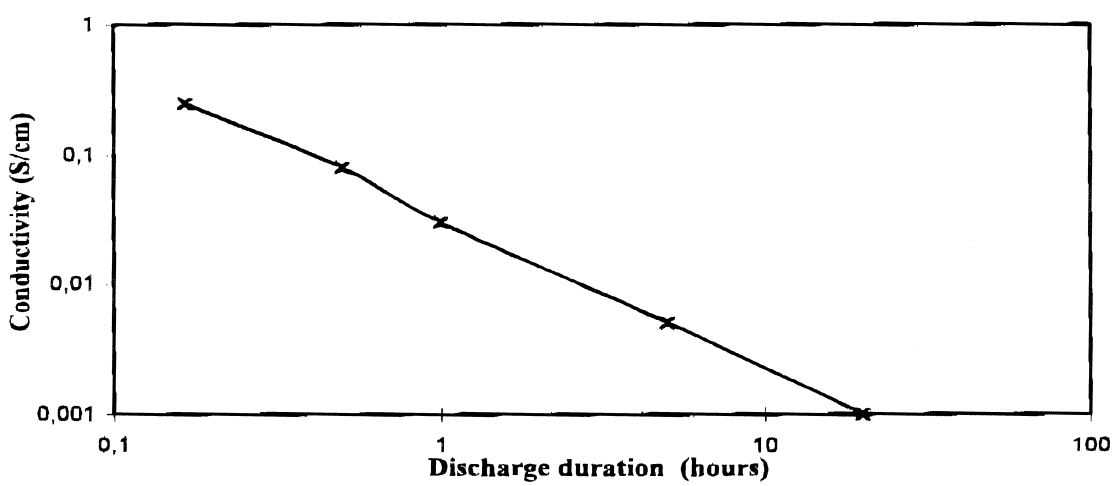

Fig. 5. Membrane conductivity for 80% available energy (compared to lead membrane) vs. discharge duration.

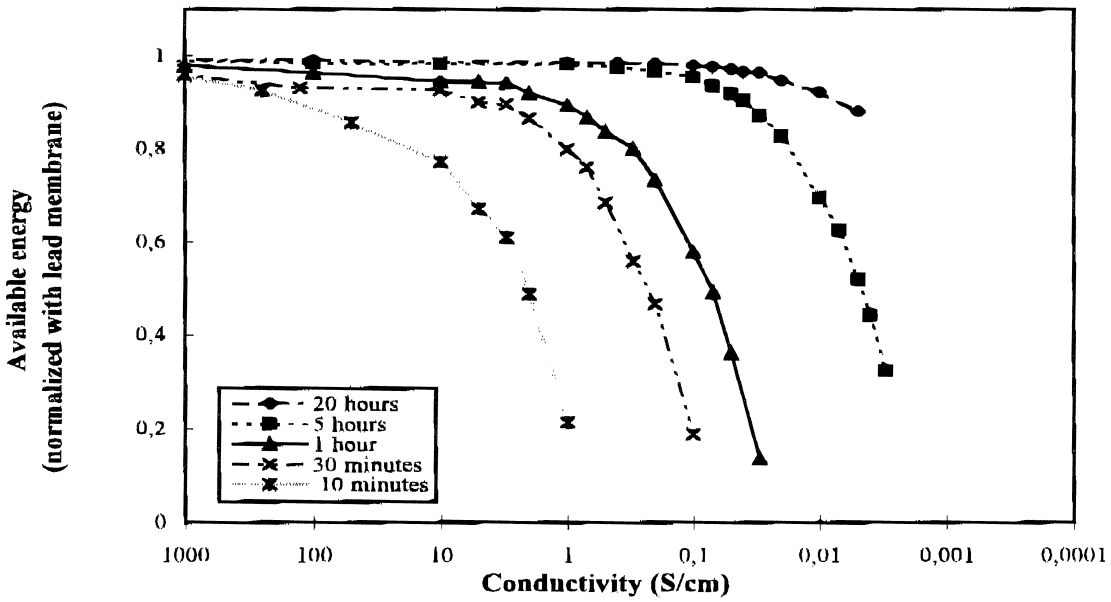

Fig. 6. Available energy vs. membrane conductivity for different rates of discharge and with composite end membranes.

6.1. Uniform voltage distribution on end plates

At first, the voltage distribution is uniform on the end plates. It is the most efficient configuration for a bipolar assembly. The prediction has been made for a 6 V cell but the result would have been the same whatever the number of cells. The energy available with a lead membrane is taken as a reference to normalize other values that have been reported in Fig. 4 for different rates of discharge.

For a discharge duration greater than 10 min, a membrane conductivity of 1 S cm^{-1} will never be performance limiting and for slower rates of discharge a membrane with a conductivity as low as 0.1 S cm^{-1} is sufficient.

The rates corresponding to a 20% decrease in available energy vs. membrane conductivity have been reported on Fig. 5. The evolution of conductivity vs. rate is linear. So it is possible to extrapolate this curve for higher discharge rates.

Nevertheless, for very high rates of discharge if the membrane conductivity is greater than the electrolyte conductivity ($\sigma_{el} < 0.76$ S cm^{-1}), the membrane conductivity will not be performance limiting and the preceding curve, which is linear, will reach an upper limit at about 10 S cm^{-1}.

6.2. Effect of end membrane conductivity

In another approach, we studied the effect of the end membrane conductivities Fig. 6. When voltage distributions are not uniform on the end membrane, the battery efficiency will increase with the number of cells, because the current distribution will become more uniform on the inner cells. As it seems interesting to study the less favourable case to really evaluate the influence of this parameter, we made the calculation for a single cell battery.

In the case of non-uniform potential distribution on the end membranes, the conductivity that avoids a loss of energy up to a 10 min discharge rate is greater than 100 S cm^{-1}. This conductivity is a hundred times higher than in the previous case.

So the current must be well distributed on the end electrodes to take advantage of the bipolar design and the conductivity of the end plates is critical.

7. Conclusions

A mathematical model was developed which can predict the voltage distribution on bipolar lead/acid batteries. It takes into account charge transfer overvoltages, diffusion effects and ohmic losses. Calculated discharge curves are in good agreement with experimental data. This model allows the influence of any parameter on discharge performances to be evaluated. Primarily, the influence of the membrane conductivity has been studied. The current must be uniformly distributed on the end membranes. Their conductivity is of prime importance because values below 100 S cm^{-1} will be performance limiting. But, providing that the current on the end plates is uniformly distributed, it appears that a conductivity of 1 S cm^{-1} is sufficient to ensure equivalent performance as for lead membranes up to a 10 min discharge rate and that a conductivity of 10 S cm^{-1} will never be performance limiting whatever the rate of discharge.

8. List of symbols

α	Transfer coefficient	
C	Concentration	mol cm^{-3}
D	Diffusion coefficient	cm^2 s^{-1}
d	density	
e	Electrode thickness	cm
ε	Porosity	
$\mathscr{E}$	Electric field	V cm^{-1}
E	Electrode potential	V
E_0	Standard electrode potential	V
F	Faraday's constant	C mol^{-1}, A s mol^{-1}
η	Electrochemical overvoltage	V
I	Total current	A
I_0	Equilibrium current	A
j	Current density	A cm^{-2}
k	Kinetic reaction constant	m s^{-1}
k_0	Kinetic standard constant	m s^{-1}
M	Molar mass	g mol^{-1}
N	Species flux	mole cm^{-2} s^{-1}
n	Number of equivalents transferred per mole of reactant	
Q	Electric capacity	A h
R	Universal gas constant	J K^{-1} mol^{-1}
S	Surface	cm^2
σ	Conductivity	S cm^{-1}
S_a	Apparent electrode area	cm^2
S_S	Specific area of the electrode	cm^2 cm^{-3}
T	Temperature	K
t	Time	h
V	Electric voltage	V
V_{el}	Electrolyte volume	cm^3
W	H_2SO_4 weight percentage	

Subscript

*	Porous material inner
a	Anodic
c	Cathodic
d	Diffusion
el	bulk electrolyte
eq	Equilibrium
H_2O	Water
H_2SO	Sulphuric acid
i	Initial
MA	Active material
max	Maximum
moy	Average
ox	Oxidant
Pb	Lead
PbO_2	Lead dioxide
red	Reductant
t	Charge transfer

References

[1] K. Wen-Hong, Computer aided design of a bipolar lead acid battery, Journal of Power Sources 36 (1991) 155–166.

[2] W.H. Tiedemann, J. Newman, Mathematical modeling of the lead acid cell, in: S. Gross (Ed.), Battery Design and Optimisation, pp. 23.

[3] K. Scott, The effect of electrode ohmic losses and the role of the electrical connection in bipolar connected parallel plate electrodes, Electrochemica Acta 28 (1983) 133–140.

[4] Z. Mao, R.E. White, Current distribution in a horizon lead acid battery during discharge, Journal of the Electrochemical Society 138 (6) (1991) 1615–1620.

[5] Y. Morimoto, Y. Ohya, K. Abe, Computer simulation of the discharge reaction in lead acid batteries, Journal of the Electrochemical Society 135 (2) (1988) 293–298.

[6] W.G. Sunu, B. Burrows, Mathematical model for design of battery electrodes. I: potential distribution, Journal of the Electrochemical Society 129 (4) (1982) 688–695.

[7] W.G. Sunu, B. Burrows, Mathematical model for design of battery electrodes. I: current density distribution, Journal of the Electrochemical Society 131 (1) (1984) 1–6.

[8] H. Bode, Lead Acid Battery, Wiley, 1977.

[9] R.M. La Follette, design fundamentals of high power density, pulsed discharge, lead acid batteries, PhD Dissertation, Brigham Young University, 1988.

[10] S. Biscaglia, Modelisation de la phase de decharge des accumulateurs au plomb. Application à la mesure de l'etat de charge, PhD Dissertation, Ecole des Mines de Paris, 1992.

[11] P. Edkunge, D. Simonsson, The discharge behaviour of the porous lead electrode in the lead-acid battery. 1: Experimental investigation, Journal of Applied Electrochemistry 19 (1989) 127–135.

[12] D. Simonsson, A mathematical model for the porous lead dioxide electrode, Journal of Applied Electrochemistry 3 (1973) 261–273.

[13] P. Edkunge, D. Simonsson, The discharge behaviour of the porous lead electrode in the lead-acid battery. 2: Mathematical model, Journal of Applied Electrochemistry 19 (1989) 127–135.

[14] M.A. Dasoyan, I.A. Aguf, Current Theory of Lead Acid Battery, Technicopy, 1979.